Karbala International Journal of Modern Science

Manuscript 3430

Green synthesis of Copper and Silver Nanostructured Particles from Eremurus Plant Extract and Comparison of their Optical Properties and Antibacterial Activities

Doaa Ayad Kamil

Ali F. Al-rawaf

Mohammed Yarub Hani

H.H. Obeed

Tabarek Falah Deindee

See next page for additional authors

Green synthesis of Copper and Silver Nanostructured Particles from Eremurus Plant Extract and Comparison of their Optical Properties and Antibacterial Activities

Abstract

In the present investigation, silver (Ag) and copper (Cu) nanostructured particles were synthesized from *Eremurus* plant by means of an environmentally benign methodology in which plant extracts served as both reducing and stabilizing agents. The resultant nanostructured particles were subjected to characterization techniques, including X-ray diffraction (XRD), Fourier-transform infrared spectroscopy (FTIR), field-emission scanning electron microscopy (FESEM), and energy-dispersive X-ray spectroscopy (EDXS). XRD analysis confirmed development of Ag nanostructured particles with face-centered cubic (*fcc*) structure and also Cu nanostructured particles with cubic form. Moreover, the average crystallite dimensions obtained for Ag and Cu were 18.3 nm and 65.7 nm, respectively. FESEM images disclosed spherical-shaped morphology of Ag alongside cubic form of Cu. The optical characteristics were scrutinized *via* UV-Visible spectroscopy, which revealed distinctive absorption peaks at 205 nm for Ag and 230 nm for Cu where Ag demonstrated a superior extinction coefficient, thereby indicated enhanced optical activity.

The antibacterial performance of Ag and Cu nanostructured particles was assessed against *Escherichia coli* (*E. coli*) and *Staphylococcus aureus* (*S. aureus*) employing the colony-forming unit (CFU) methodology. Ag nanostructured particles exhibited remarkable antibacterial efficacy, achieving a reduction exceeding 99.99999% against *E. coli* and over 99.999% against *S. aureus* at a concentration of 8 mg/mL. Cu nanostructured particles similarly manifested substantial antibacterial effects, diminishing *E. coli* populations by over 99.99999% and *S. aureus* by greater than 99.98% at a concentration of 0.3 mg/mL. The augmented antimicrobial properties of Ag and Cu nanostructured particles underscored their prospective applications in biomedical, environmental, and antimicrobial coating domains.

Keywords

Silver nanostructured particles; Copper nanostructured particles; Green synthesis; Antibacterial activity; Optical properties; E. coli; S. aureus

Authors

Doaa Ayad Kamil, Ali F. Al-rawaf, Mohammed Yarub Hani, H.H. Obeed, Tabarek Falah Deindee, and Mohammed Ridha Shaeed

RESEARCH PAPER

Green Synthesis of Copper and Silver Nanostructured Particles From *Eremurus* Plant Extract and Comparison of Their Optical Properties and Antibacterial Activities

Doaa A. Kamil [a], Ali F. Al-rawaf [b,c], Mohammed Y. Hani [d,*], Hawra H. Obeed [b], Tabarek F. Deindee [e], Mohammed R. Shaeed [f]

[a] Department of Science, Branch Physics, College of Basic Education, University of Sumer, Dhi Qar, Iraq
[b] Department of Physics, College of Education for Pure Science, University of Kerbala, Karbala, Iraq
[c] Department of Anesthesia Techniques, Alsafwa University College, Karbala, Iraq
[d] Department of Environmental Health, College of Applied Medical Science, University of Kerbala, Karbala, Iraq
[e] Department of Physics, College of Science, University of Babylon, Babylon, Iraq
[f] Department of Laser Physics, College of Science for Women, University of Babylon, Babylon, Iraq

Abstract

In the present investigation, silver (Ag) and copper (Cu) nanostructured particles were synthesized from *Eremurus* plant by means of an environmentally benign methodology in which plant extracts served as both reducing and stabilizing agents. The resultant nanostructured particles were subjected to characterization techniques, including X-ray diffraction (XRD), Fourier-transform infrared spectroscopy (FTIR), field-emission scanning electron microscopy (FESEM), and energy-dispersive X-ray spectroscopy (EDXS). XRD analysis confirmed development of Ag nanostructured particles with face-centered cubic (*fcc*) structure and also Cu nanostructured particles with cubic form. Moreover, the average crystallite dimensions obtained for Ag and Cu were 18.3 nm and 65.7 nm, respectively. FESEM images disclosed spherical-shaped morphology of Ag alongside cubic form of Cu. The optical characteristics were scrutinized *via* UV-Visible spectroscopy, which revealed distinctive absorption peaks at 205 nm for Ag and 230 nm for Cu where Ag demonstrated a superior extinction coefficient, thereby indicated enhanced optical activity.

The antibacterial performance of Ag and Cu nanostructured particles was assessed against *Escherichia coli* (*E. coli*) and *Staphylococcus aureus* (*S. aureus*) employing the colony-forming unit (CFU) methodology. Ag nanostructured particles exhibited remarkable antibacterial efficacy, achieving a reduction exceeding 99.99999 % against *E. coli* and over 99.999 % against *S. aureus* at a concentration of 8 mg/mL. Cu nanostructured particles similarly manifested substantial antibacterial effects, diminishing *E. coli* populations by over 99.99999 % and *S. aureus* by greater than 99.98 % at a concentration of 0.3 mg/mL. The augmented antimicrobial properties of Ag and Cu nanostructured particles underscored their prospective applications in biomedical, environmental, and antimicrobial coating domains.

Keywords: Silver nanostructured particles, Copper nanostructured particles, Green synthesis, Antibacterial activity, Optical properties, *E. coli*, *S. aureus*

1. Introduction

Nanotechnology has fundamentally transformed multiple scientific disciplines, including but not limited to medicine, environmental science, and materials engineering, by facilitating the synthesis and utilization of nanoparticles possessing distinctive physicochemical

Received 10 June 2025; revised 23 August 2025; accepted 26 August 2025.
Available online 23 September 2025

* Corresponding author.
E-mail address: mohammed.yaareb@uokerbala.edu.iq (M.Y. Hani).

https://doi.org/10.33640/2405-609X.3430

attributes. Among the diverse array of nanomaterials, metal and metal oxide nanoparticles have attracted considerable scholarly interest due to their exceptional antibacterial properties, biocompatibility, and prospective applications in industries, healthcare section, and environmental remediation [1−4]. Silver (AgNPs) and copper (CuNPs) nanoparticles are among the most extensively investigated nanomaterials, which is attributed to their potent antimicrobial characteristics, economic viability, and the feasibility of their synthesis through environmentally sustainable methods [5,6]. The prevalence of bacterial infections, particularly those instigated by multidrug-resistant (MDR) strains, constitutes a significant global health challenge, thereby necessitating the formulation of alternative antimicrobial agents. The efficacy of conventional antibiotics has been diminished due to the rise of MDR bacteria, leading to comprehensive investigations on nanomaterials as potential antibacterial alternatives [7]. Ag and Cu nanoparticles have exhibited remarkable antibacterial efficacy against different Gram-positive and Gram-negative bacteria, for instance *E. coli*, *S. aureus*, *Pseudomonas aeruginosa* (*P. aeruginosa*), and *Staphylococcus epidermidis* (*S. epidermidis*), which could make them promising candidates for biomedical applications [8,9]. Nevertheless, there exists a paucity of comprehensive comparative analyses regarding their antibacterial effectiveness when employing a green synthesis methodology.

In spite of their drawbacks for instance being time-consuming, loss of part of the extract, and the contamination of the resulting product with organic solvents, the green synthesis of nanoparticles entails the utilization of phytochemical extracts, microorganisms, or alternative biological systems as reducing and stabilizing agents, thereby presenting an environmentally benign alternative to traditional chemical and physical synthesis methodologies. Moreover, it diminishes the reliance on hazardous and toxic chemicals and fosters biocompatibility, rendering it a sustainable option for the fabrication of nanoparticles [10,11].

Numerous plant extracts are endowed with bioactive constituents, including polyphenols, flavonoids, and alkaloids, which facilitate the reduction of metal salts into nanoparticles while concurrently augmenting their stability and biological efficacy [12,13]. The green synthesis technique has been extensively employed for the generation of Ag and Cu nanoparticles characterized by high purity and regulated physicochemical properties, factors that can significantly affect their antibacterial performance [14,15]. In this regard, Assad and his co-workers prepared AgNPs by means of the polar extract of *Cotoneaster nummularius* leaves and their optical and antimicrobial properties were examined using various techniques. The presence of the absorption band related to surface plasmon resonance (SPR) of AgNPs in their ultraviolet (UV-Visible) spectrum and also the peak showing AgNPs in their FTIR spectrum supported their successful fabrication. The synthesized nanostructures exhibited potent antimicrobial activity against several bacterial and fungal strains, which resulted in their comparable wound healing results with commercial Sufre tulle® dressing [16]. In another study, CuNPs were prepared by means of the root extract of *Withania somnifera* and their antibacterial activities were examined against *Escherichia coli* (*E. coli*) and *Staphylococcus aureus* (*S. aureus*). The resulting CuNPs revealed higher antibacterial activity against *S. aureus* compared to *E. coli*. Moreover, in accordance with antioxidant activities results obtained from DPPH assay, the inhibition percentage of NPs was 62 % at the concentration of 400 μg/mL [17].

AgNPs are renowned for their potent antibacterial properties, which arise from various mechanisms, including disruption of cell membranes, induction of oxidative stress, and interaction with bacterial proteins and DNA [18]. These mechanisms underpin the efficacy of AgNPs against both gram-positive and gram-negative bacteria, thereby rendering them invaluable for antimicrobial applications [19]. Furthermore, AgNPs demonstrate a broad spectrum of antimicrobial activity, limited development of resistance, and promising applications in medical coatings, wound dressings, metal ion sensing, and water purification systems [20−22]. CuNPs as well as AgNPs exhibit significant antibacterial capabilities mainly attributable to their propensity to generate reactive oxygen species (ROS), ability to release ions, and contact killing properties [23]. ROS species generated by NPs include oxygen-containing radicals and non-radicals. Some of the negative ROS, for instance OH^- are inclined to have interaction with positively charged membranes of microbial cells. On the other hand, neutral ROS are prone to penetrate the cell membranes. The ability of nanoparticles to release ions is another reason behind their antimicrobial activity. The ions transported and delivered by NPs could penetrate membrane of the bacterial cells and influence their DNA, RNA, and transcriptional responses. Unlike two aforementioned mechanisms where NPs indirectly involve in destruction of the microbial cells (either by generated ROS or release of ions), in contact killing, NPs directly interact with membrane of the cells and penetrate into them [23].

The antimicrobial applications of CuNPs have been extensively explored, particularly in the contexts of coatings, packaging materials, and biomedical devices [24]. In comparison with AgNPs, CuNPs are deemed more economically viable and offer additional advantages, including potential antifungal and antiviral attributes [25]. Nonetheless, disparities in their antibacterial efficacy, toxicity profiles, and stability necessitate further examination to ascertain their appropriateness for diverse applications [26].

Notwithstanding the comprehensive investigations into silver and copper nanoparticles, a direct comparative evaluation of their antibacterial characteristics utilizing a green synthesis methodology remains insufficiently examined. This research endeavors to synthesize silver and copper nanostructured particles employing *Eremurus* plant extracts and assess their antibacterial efficacy against *E. coli* and *S. aureus*. Using *Eremurus* extract possesses several advantages, one of which is that it is natural. In addition to its antibacterial characteristics, it shows antioxidant, cytotoxic, and antidiabetic properties, which could provide a wider range of applications. Moreover, it has traditionally been used for treatment of different health issues [13].

The physicochemical attributes of the nanostructured particles are characterized utilizing X-ray diffraction (XRD), Fourier-transform infrared spectroscopy (FTIR), field emission scanning electron microscopy (FESEM), and energy dispersive X-ray spectroscopy (EDXS). Furthermore, their optical characteristics are scrutinized through UV-Visible spectroscopy. The antibacterial effectiveness is evaluated employing the colony-forming unit (CFU) methodology to ascertain their potential as alternative antimicrobial agents. We expected that synthesized Ag and Cu nanostructured particles from *Eremurus* plant would exhibit high antibacterial activities against *E. coli* and *S. aureus*. Hence, the outcomes of this investigation would yield significant insights into the comparative performance of silver and copper nanostructured particles, thereby contributing to their prospective applications in biomedical, environmental, and antimicrobial technologies.

2. Experimental section

2.1. Green synthesis of silver nanostructured particles

The fabrication of Ag nanostructured particles was executed utilizing an environmentally benign methodology involving an aqueous extract derived from *Eremurus* (Isfahan, Iran). Initially, 50 gr of *Eremurus* were meticulously ground and subsequently dissolved in 200 mL of deionized water. This resultant mixture was permitted to stand for a duration of 24 h, after which the extract was segregated from the solid residues. The resulting solution was subjected to continuous stirring and heating at 80 °C for a period of 1 h, followed by filtration to eradicate any remaining particulates.

Thereafter, 0.1 moles of silver nitrate ($AgNO_3$) were dissolved in 100 mL of deionized water. The previously prepared *Eremurus* extract was then incrementally introduced into the $AgNO_3$ solution under sustained stirring, thereby promoting the formation of a precipitate. The reaction mixture was allowed to mature at ambient temperature for 6 h, culminating in the emergence of a brown precipitate, which is indicative of Ag nanostructured particles formation. The resultant precipitate was subsequently filtered and rigorously washed several times with deionized water and ethanol to remove any residual impurities. Ultimately, the purified precipitate was subjected to drying at 60 °C in preparation for ensuing characterization analyses.

2.2. Green synthesis of copper nanostructured particles using aqueous extract of Eremurus

The eco-friendly synthesis of Cu nanostructured particles was executed utilizing an aqueous extract derived from the *Eremurus* plant. In this regard, 50 g of Fresh *Eremurus* was carefully chopped and subsequently, amalgamated with 200 mL of deionized water. Then, the resultant mixture was allowed to repose for 24 h to facilitate the extraction of bioactive compounds. The extract was subsequently agitated at a moderate temperature for 1 h to augment the extraction efficiency.

After that, the resultant solution underwent filtration using filter paper to eliminate solid residues. The aqueous extract was incrementally introduced into a copper nitrate ($Cu(NO_3)_2$) solution under continuous agitation until a discernible color change and precipitate formation were noted.

The reaction mixture was permitted to stand for 6 h to guarantee the completion of precipitation. The precipitate was isolated *via* centrifugation at 7000 rpm and subsequently subjected to multiple washings with deionized water and ethanol to eliminate impurities. Finally, the purified precipitate was dried at 60 °C and further subjected to annealing under a medium vacuum (40 Torr) within a temperature range of 350−400 °C to eradicate excess organic constituents and yield the final Cu nanostructured particles.

The synthesized nanostructured particles were then characterized employing various analytical techniques to assess their structural, morphological, and antibacterial properties.

2.3. Characterization analyses

The crystal structures of the prepared Ag and Cu nanostructured particles were scrutinized with an EQUINOX 3000 Intel X-ray diffractometer using Cu-Kα radiation ($\lambda = 0.15418$ nm). For investigation of the organic and inorganic bonds inside the synthesized nanostructured particles, a Bruker Alpha Fourier transform infrared (FT-IR) spectrometer was adopted. The morphology as well as chemical composition of Ag and Cu nanostructures were respectively studied by means of FESEM instrument (Tescan Mira 3-LMU, 15 kV) and an energy dispersive spectrometer (EDS) mounted on it. The UV-Visible measurements were performed by Perkin Elmer Lambda 45 spectrometer.

2.4. Antibacterial activity assessment

Two bacterial strains, consisting of *E. coli* ATCC25922 and *S. aureus* ATCC 6598 were chosen for the analysis of antibacterial activity of Ag and Cu nanostructured particles. Both bacteria were cultured in the medium of the Müller-Hinton-agar, followed by incubating for 24 h at 37 °C. The bacterial suspension of each strain was adjusted at 0.5 McFarland and a consistent volume of 1 mL of each strain was used to inoculate nutrient agar plates.

3. Results and discussion

3.1. Characterization analyses

Figure 1 demonstrates the XRD patterns of Ag and Cu nanostructured particles taken in the 2θ ranging from 10 to 80°. The crystallographic study of nanostructured particles is typically carried out by means of XRD spectroscopy. Moreover, the crystalline size of the nanostructures can be determined with the aid of this technique.

According to XRD pattern of Ag nanostructured particles, the main peaks found at 2θ of 38.1, 44.3, and 64.4° are attributed to the crystal planes of (111), (200), and (220), respectively (JCPDS file No. 04-0783). The aforementioned XRD peaks demonstrate the face-centered cubic (*fcc*) structure of Ag nanostructured particles [1,4]. No other peak except for the ones seen in the XRD pattern of Ag can be

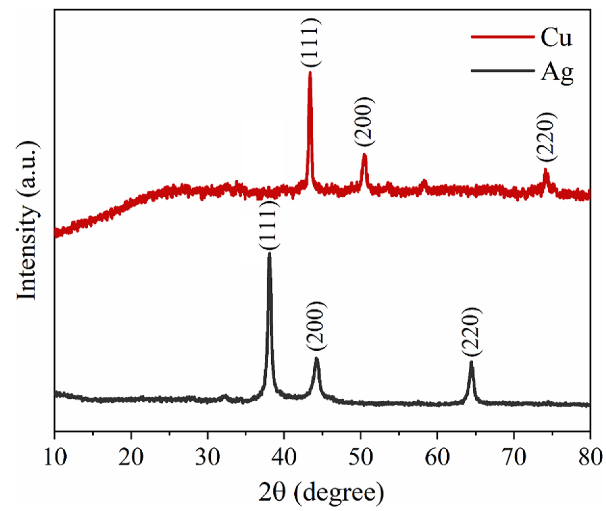

Fig. 1. The XRD patterns of Ag and Cu nanostructured particles within the range of 10–80°.

found, meaning that our fabricated nanostructured particles lack of any contaminant and possess high purity. The crystalline size of Ag nanostructured particles was estimated using the following formula, known as Debye–Scherrer's equation [5,27]:

$$D = \frac{K\lambda}{\beta \cos\theta} \tag{1}$$

Where D signifies the mean size of the nanostructured particles, K indicates the Scherrer constant (K = 0.98), λ denotes the wavelength of X-ray equal to 1.541 Å, and β demonstrates the full width at half maximum (FWHM). By taking the sharpest peak at 38.1° into account for calculation of average crystalline size of Ag nanostructured particles, a value of 18.3 nm is obtained for this sample.

For the Cu nanostructured particles (Figure 1), three diffraction peaks can be detected at 2θ of 43.4, 50.4, and 74.1°. Based on JCPDS file No. 04-014-0265, the aforementioned peaks are indications of Miller indices of (111), (200), and (220), respectively, which suggest a cubic structure for our prepared Cu nanostructured particles [6,28]. By employing Equation (1), an average crystalline size of 65.7 nm is estimated for Cu nanostructured particles. FTIR technique is another characterization analysis hired to structurally examine the fabricated Ag and Cu nanostructured particles. FTIR is advantageous because of its capability to scrutinize the functional groups available within the prepared nanostructured particles.

Based on references, the Ag nanostructured particles synthesized from plant extract contain different functional groups for example amines, alcohols, and so on [29]. In this direction and in accordance with Figure 2 showing the FTIR spectrum of Ag nanostructured particles, a broad peak can be detected at about 3200 cm^{-1}, which corresponds to stretching mode of O−H functional group within alcohols or N−H in amines [7,29]. The O−H absorption band can also be originated from the presence of water molecules [1]. Another well-defined peak is seen at 1562 cm^{-1}, which is pertinent to the stretching mode of C=O overlapped with amine-bending vibration [5,30]. The peaks found at the wavenumbers of 1382 and 1014 cm^{-1} are arisen from the primary amide groups and C−O in ethers, respectively [7].

In terms of FTIR spectrum of Cu nanostructured particles (Figure 2), the broad peak at 3424 cm^{-1} corresponds to stretching vibration of O−H in alcohol and phenols [6,8]. The pronounced peak at 1577 cm^{-1} is relevant to the stretching mode of C=O [10]. The peak at 1054 cm^{-1} is related to C−O in ethers [6].

To evaluate morphology of the prepared Ag and Cu nanostructured particles, FESEM is adopted. According to references, Ag nanostructured particles prepared from plant extract typically appear in the form of hexagonal, spherical or triangular [31]. As shown by FESEM image of Ag nanostructured particles (Figure 3a), a mass of spherical-shaped nanostructured particles of silver are evident whose size is approximately in the range of 50−100 nm (Figure 3b). For the Cu nanostructured particles, the cubic-shaped species dispersed within an interconnected network are observed (Fig. 3c and d), which are correlated to copper particles. The size of Cu nanostructured particles is estimated at about 500 nm.

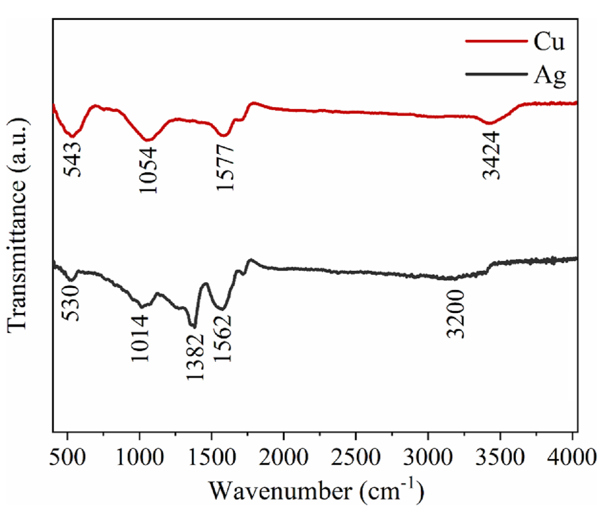

Fig. 2. The FTIR spectra of Ag and Cu nanostructured particles.

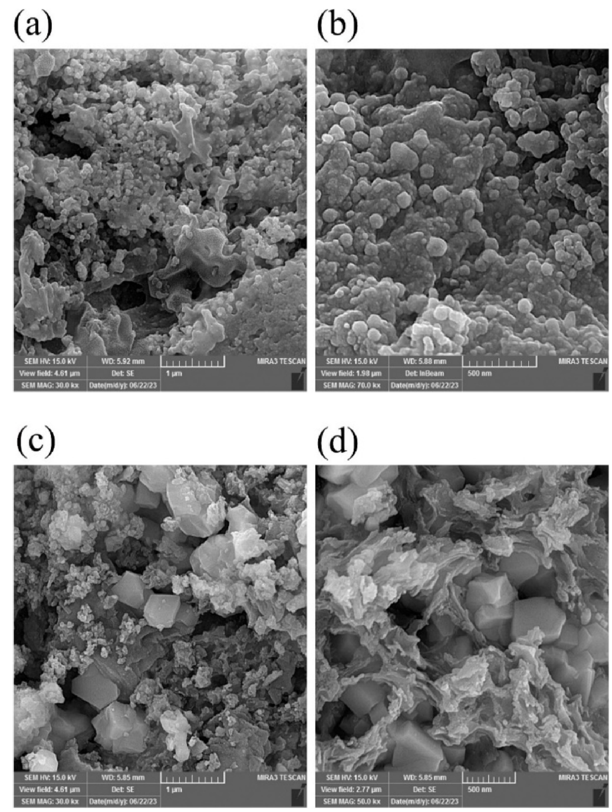

Fig. 3. The FESEM images of (a,b) Ag and (c,d) Cu nanostructured particles at various magnifications.

EDXS is employed to probe the elemental composition of fabricated Ag and Cu nanostructured particles. According to Figure 4a exhibiting the EDXS pattern of Ag nanostructured particles, the two characteristic peaks of Ag element found at about 3 keV are arisen from the silver particles. For the Cu nanostructured particles, the pronounced peaks of Cu element at approximately 0.9, 8, and 8.9 keV (Figure 4b) testify the presence of copper particles.

3.2. Optical behavior investigation

In order to investigate optical properties of Ag and Cu nanostructured particles, UV-Visible absorption spectroscopy is adopted. Figure 5a illustrates the UV-Visible spectra of Ag nanostructured particles. Accordingly, a sharp absorption peak can be detected at approximately 205 nm for this sample, which is located in the UV region. Like Ag, the UV-Visible spectrum of Cu nanostructured particles demonstrates only one absorption peak, which is centered at about 230 nm (Figure 5a). Compared to Ag, the absorption peak of Cu nanostructured particles shifts toward higher wavelength, meaning that a redshift is observed.

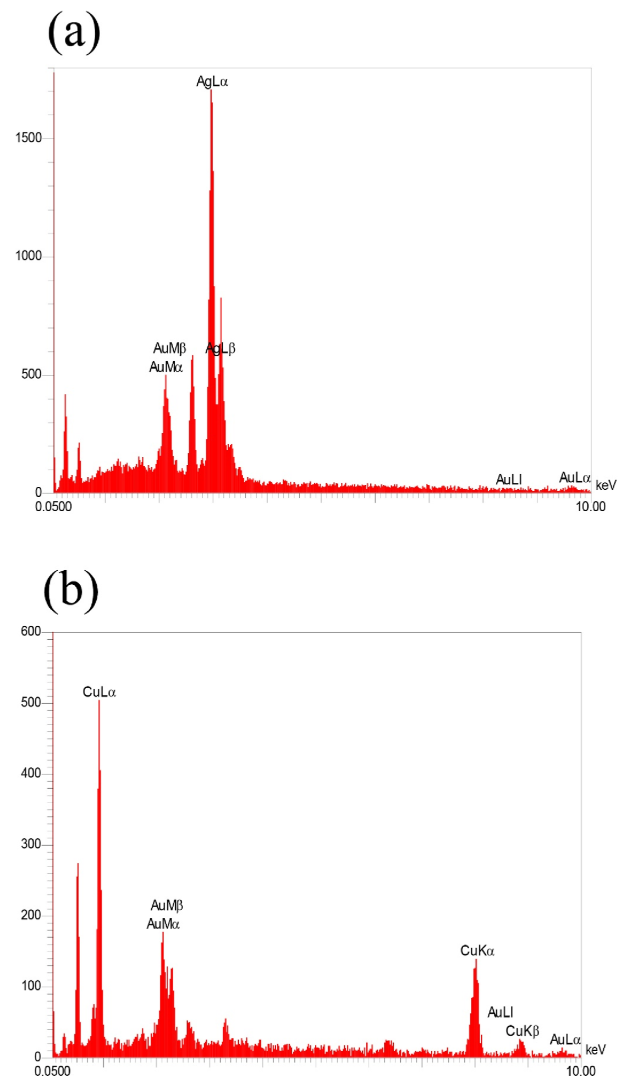

Fig. 4. The EDXS patterns of (a) Ag and (b) Cu nanostructured particles.

In order to obtain the energy band gap of Ag and Cu nanostructured particles, their Tauc's plots are plotted (Figure 5b). For this purpose, the straight line acquired from plotting $(\alpha h\nu)^2$ versus photon energy ($h\nu$) is extrapolated to horizontal axis, by which an estimated energy band gap (E_g) can be obtained. In this regard, α demonstrates the absorption coefficient of the material, h indicates the Planck's constant, and ν signifies the frequency of the light [12,32].

The energy band gap calculated for Ag and Cu nanostructured particles respectively is 5.6 and 3.8 eV. The lower energy band gap means the shorter distance between the valance band and conduction band, which simplifies the transition of electrons between two bands. The transmittance spectra of Ag and Cu nanostructured particles as a function of wavelength are shown in Figure 6. The transmittance percentage (T%) was calculated by means of the following equation [33]:

$$T\% = 100 \times 10^{-A} \tag{2}$$

Where A shows absorbance. Accordingly, the peaks at 205 nm for Ag and at 230 nm for Cu nanostructured particles found in their absorbance spectra (Figure 5a) are also observed in their transmittance spectra. Moreover, the redshift seen for the Cu nanostructured particles in their absorbance spectrum is also detected in their transmittance spectra. Compared to Cu, Ag nanostructured particles exhibit less transmittance, which is consistent with absorption spectroscopy where they showed higher intensity.

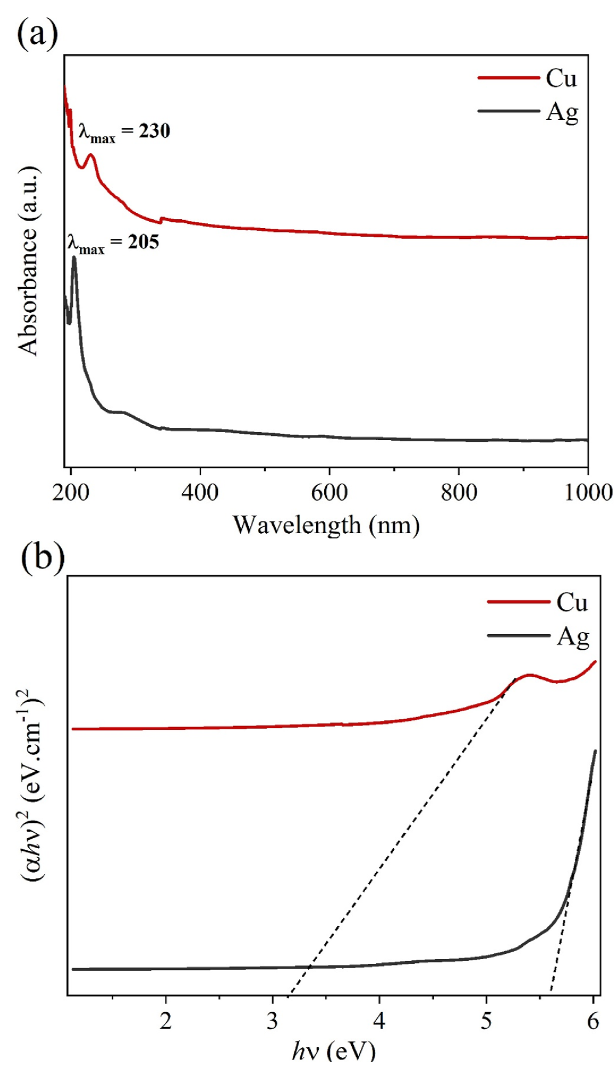

Fig. 5. (a) The absorbance spectra and (b) energy band gap of Ag and Cu nanostructured particles.

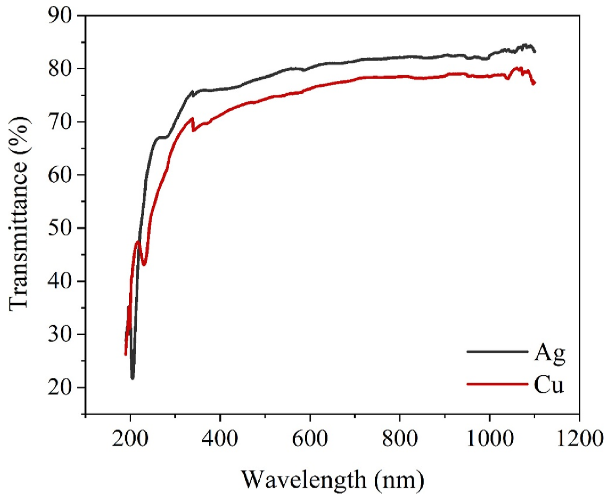

Fig. 6. The transmittance spectra of Ag and Cu nanostructured particles.

Figure 7 demonstrates the extinction coefficient versus wavelength curves for Ag and Cu nanostructured particles. Equation (3) is adopted for calculation of extinction coefficients (K) of the samples [34]:

$$K = \frac{\alpha\lambda}{4\pi} \quad (3)$$

In Equation (3), α is the absorption coefficient and λ demonstrates the wavelength. In accordance with Figure 7, Ag nanostructured particles show higher extinction coefficient compared to Cu, implying higher capability of Ag in absorbing the light.

In addition to extinction coefficient, the refractive indexes (n) of Ag and Cu nanostructured particles versus wavelength are obtained, which are demonstrated by Figure 8. The calculation of refractive indexes is carried out by means of Equation (4) [30]:

$$n = \frac{1}{T_s} + \sqrt{\frac{1}{T_s^2 - 1}} \quad (4)$$

Where T denotes transmittance. Accordingly, the refractive index exhibited by Ag nanostructured particles is about 0.05, which is lower than the one obtained for Cu, which is 0.45. Lower refractive index means the property of a material in reducing the reflection of light. Higher extinction coefficient and lower refractive index of Ag nanostructured particles in comparison with Cu are in a well agreement with their higher absorption and lower transmittance, which make them appropriate for optical activities. Higher capability of Ag compared to Cu in absorbing the light can be arisen from their smaller dimension, as confirmed by XRD and FESEM analyses, which provides larger surface-to-volume ratio.

3.3. Antibacterial activities

The antibacterial activities of Ag and Cu nanostructured particles are examined against *E. coli* and *S. aureus* bacteria where colony forming unit (CFU) parameter, which determines the number of viable bacteria in a sample, is adopted for this purpose. Figs. 9 and 10 respectively demonstrate antibacterial activities of control sample (negative-type) and silver nanostructures against *E. coli* bacteria as a gram-negative bacterium. Besides, the CFU values acquired for the control sample and also Ag

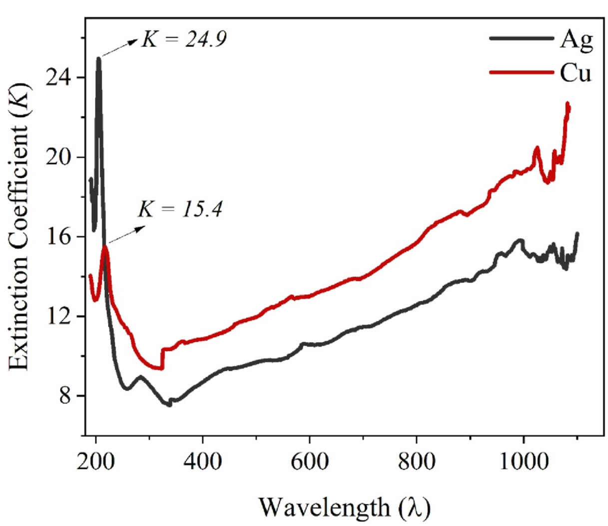

Fig. 7. The extinction coefficient of Ag and Cu nanostructured particles.

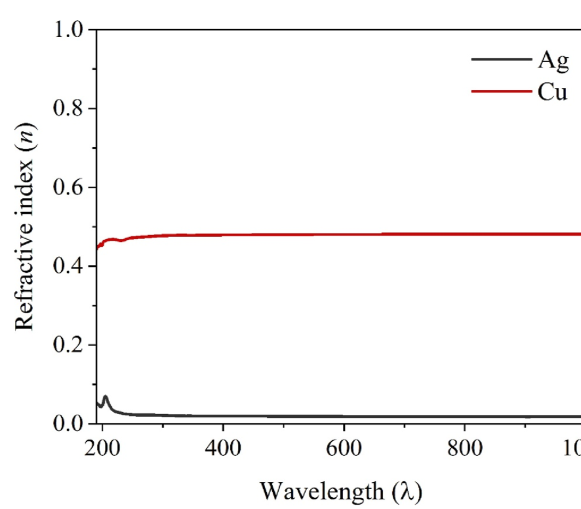

Fig. 8. The refractive index versus wavelength curves for Ag and Cu nanostructured particles.

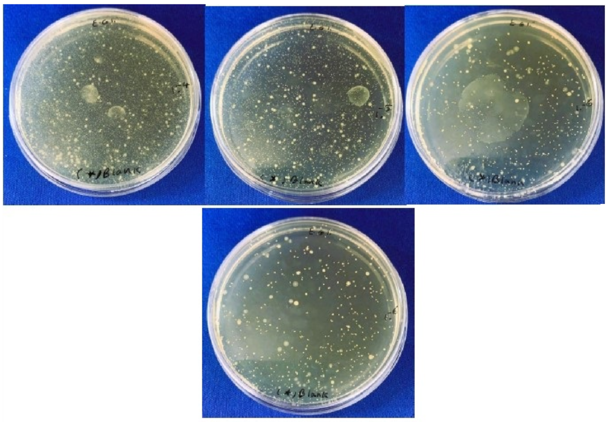

Fig. 9. Antibacterial activity of control sample against E. coli bacteria after 24-h incubation.

nanostructures before and after 24-h contact are brought in Table 1.

In this direction, the CFU value shown by control sample before contact is 1.78×10^5 mL. On the other hand, and after 24-h contact, this value reaches 3.22×10^8 mL, showing that no reduction is seen in the number of *E. coli* bacteria and the control sample exhibits no antibacterial activity (Figure 9).

Regarding Ag nanostructures, the CFU value of 1.78×10^5 mL is obtained before the contact. But and after 24-h contact, the number of *E. coli* bacteria decreases to less than 10 mL corresponding to a reduction of >99.99999 %, attesting that Ag nanostructures manifest significant antibacterial activity against *E. coli* (Figure 10).

In addition to *E. coli*, the antibacterial activities of control sample as well as Ag nanostructures were examined against *S. aureus* as a gram-positive bacterium. In this regard, the control sample reaches a CFU value of 3.1×10^5 mL before contact (Table 1). However, this value increases to 1.8×10^6 mL after 24-h contact, demonstrating that no reduction seen in the number of *S. aureus* bacteria and the control sample exhibits no antimicrobial activity (Figure 11). Ag nanostructures show considerable antibacterial activities against *S. aureus* bacteria. In this regard, the CFU value of the Ag nanostructures before contact is 3.1×10^5 mL (Table 1).

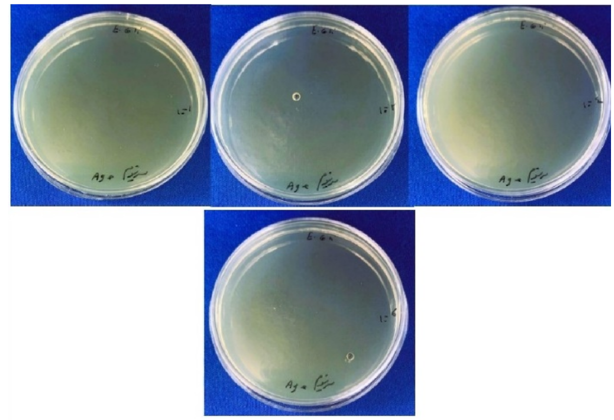

Fig. 10. Antibacterial activity of Ag nanoparticles against E. coli bacteria after 24-h incubation.

After 24-h contact with Ag nanostructured particles, CFU declines to less than 10 mL and a reduction of >99.999 % is observed in the number of *S. aureus* bacteria (Figure 12). As a consequence, Ag nanostructured particles possess high antibacterial activities against both *E. coli* and *S. aureus* bacteria.

Accordingly, the CFU value obtained for the control sample before contact with *E. coli* bacteria is 1.78×10^5 mL. On the other hand, this parameter increases to 3.22×10^8 mL after 24-h contact;

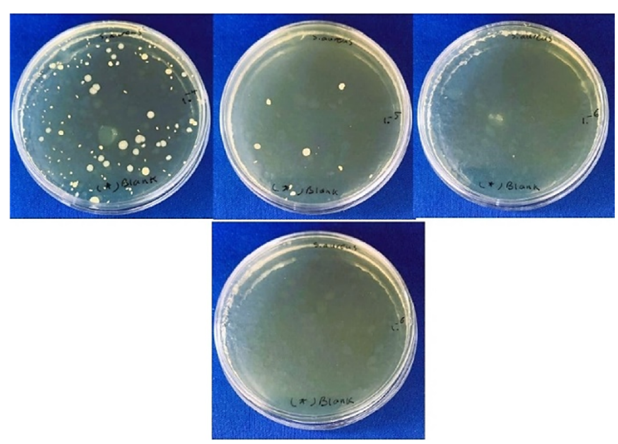

Fig. 11. Antibacterial activity of control sample against S. aureus bacteria after 24-h incubation.

Table 1. Antibacterial activities of Ag nanostructures against E. coli and S. aureus bacteria.

Microorganism	Sample	CFU (mL) (before contact)	Sample Concentration (mg/mL)	CFU (mL) (after 24-h contact)	Reduction (%)
Escherichia coli	Ag	1.78×10^5	8	<10	>99.99999
	Control		8	3.22×10^8	–
Staphylococcus aureus	Ag	3.1×10^5	8	<10	>99.999
	Control		8	1.8×10^6	–

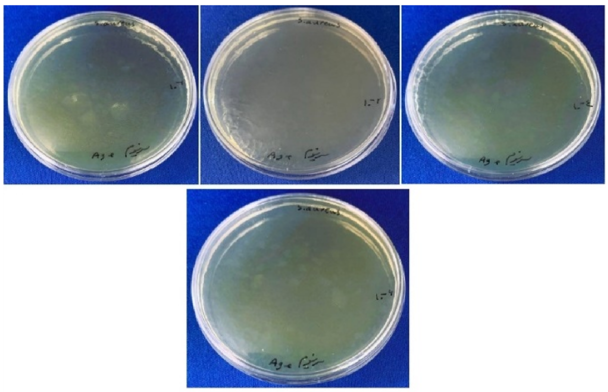

Fig. 12. Antibacterial activity of Ag nanostructured particles against S. aureus bacteria after 24-h incubation.

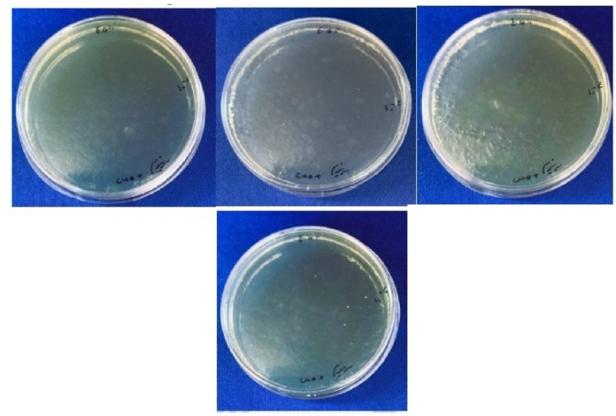

Fig. 14. Antibacterial activity of Cu nanostructures against E. coli bacteria after 24-h incubation.

therefore, no decrement is seen in the number of *E. coli* bacteria and the control sample exhibits no antibacterial activity (Figure 13).

However, Cu nanostructured particles demonstrate high antibacterial activities against *E. coli* bacteria. Accordingly, the CFU value before contact with Cu nanostructured particles is 1.78×10^5 mL (Table 2). After 24-h exposure with Cu, the CFU decreases to less than 10 mL, which corresponds to a reduction of more than >99.99999 (Figure 14).

The antibacterial activity of Cu nanostructured particles is also examined against gram-positive bacterium of *S. aureus*. In this regard, the control sample demonstrates no antibacterial activity against *S. aureus* (Figure 15). The CFU values obtained for the control sample before and after 24-h contact respectively are 3.1×10^5 and 1.8×10^6 mL (Table 2); thus, no reduction occurred in the number of *S. aureus* bacteria.

However, exposure of *S. aureus* bacteria to Cu nanostructured particles gives rise to a significant decrement in their number (Figure 16).

According to Table 2, the CFU value before contact is 3.1×10^5 mL. After 24-h contact, this

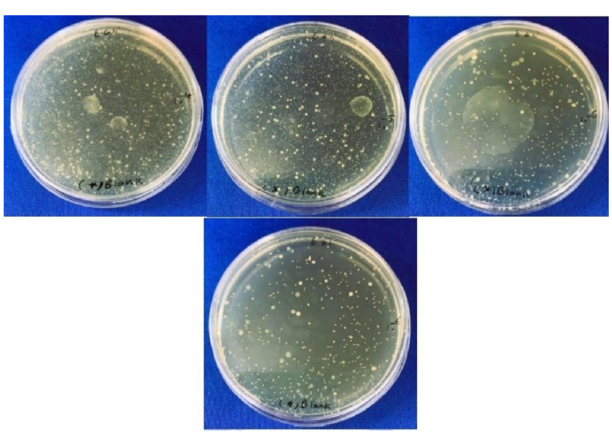

Fig. 13. Antibacterial activity of control sample against E. coli bacteria after 24-h incubation.

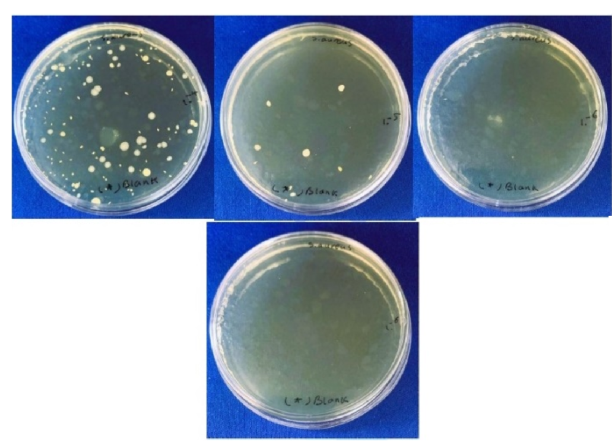

Fig. 15. Antibacterial activity of control sample against S. aureus bacteria after 24-h incubation.

Table 2. Antibacterial activities of Cu nanostructures against E. coli and S. aureus bacteria.

Microorganism	Sample	CFU (mL) (before contact)	Sample Concentration (mg/mL)	CFU (mL) (after 24-h contact)	Reduction (%)
Escherichia coli	Cu	1.78×10^5	0.3	<10	>99.99999
	Control		–	3.22×10^8	–
Staphylococcus aureus	Cu	3.1×10^5	0.3	3.8×10^2	>99.98
	Control		–	1.8×10^6	–

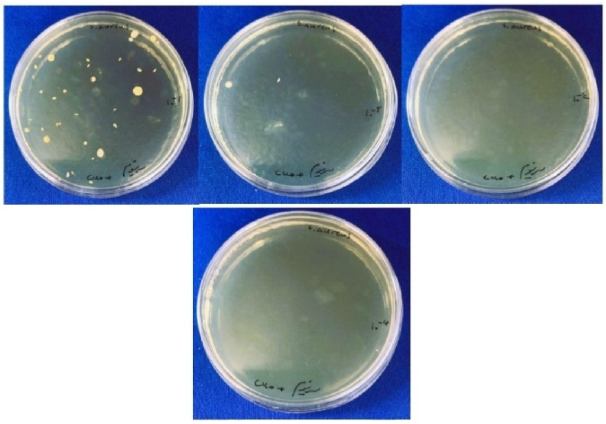

Fig. 16. Antibacterial activity of Cu nanostructured particles against S. aureus bacteria after 24-h incubation.

value decreases to 3.8×10^2 mL, which corresponds to a reduction of >99.98 %. As a result, Cu nanostructures show high antibacterial activities against both gram-negative and gram-positive bacteria. The comparison between Tables 1 and 2 shows that Ag outperforms Cu against gram-positive bacteria, which originates from several mechanisms, including direct contact to the membranes of the bacteria and their destruction, production of ROS species, denaturation of enzymes in bacteria, interruption in cellular redox reactions in bacteria, and damages to critical cellular components of bacteria for instance DNA and RNA [35,36]. However, both Ag and Cu reveals excellent antimicrobial activity. As evidenced by XRD spectroscopy, both Ag and Cu demonstrated high crystallinity, which could result in their high antibacterial activity due to presence of negligible amorphous phases. Moreover, in accordance with FESEM images, Ag and Cu appeared in nanometer size, which could provide higher surface-to-volume ratio and subsequently, more active size for release of their corresponding ions [37,38].

4. Conclusions

In this work, Ag and Cu nanostructured particles were synthesized from plant extract and their optical properties and also antibacterial activities were scrutinized by means of various analyses.

As all the characterization tests of XRD, FTIR, FESEM, and EDXS corroborated, Ag and Cu nanostructured particles were successfully prepared. In accordance with XRD technique, Ag and Cu respectively showed face-centered cubic (*fcc*) and cubic structure. Both samples revealed different morphologies where spherical-shaped nanostructured particles and cubic-shaped species were respectively observed for Ag and Cu. In EDXS patterns of Ag and Cu nanostructures, the peaks of silver and copper elements were detected, which confirmed further our case-study samples. Although Ag nanostructured particles showed higher energy band gap compared to Cu nanostructures, they were found to be more effective in optical behavior examinations. In this regard, Ag nanostructured particles manifested higher absorption, lower transmittance, more extinction coefficient and less refractive index in comparison with Cu. High optical properties of Ag nanostructures were related to their smaller dimensions. Both Ag and Cu nanostructured particles took advantage of excellent antibacterial activities against both gram-negative and gram-positive bacteria where Ag showed better antibacterial activity against gram-positive bacteria compared to Cu.

Our findings suggest that Ag and Cu nanostructured particles are potential for photocatalytic applications, including environmental remediation applications, energy conversion uses, and green synthesis of chemicals. Additionally, both can be used to overcome the health issues generated by *E. coli* and *S. aureus* bacteria.

Ethics information

This study did not involve human participants or animal subjects, and therefore ethical approval was not required.

Funding

This research did not receive any specific grant from funding agencies in the public, commercial, or not-for-profit sectors. All expenses were covered by the author personally.

Conflicts of interest

The authors declare that they have no competing interests.

Acknowledgements

The authors would like to express their gratitude to the contributing universities for their moral support and for providing laboratory resources essential to the completion of the practical component of this research.

References

[1] D. Garibo, H.A. Borbón-Nuñez, J.N.D. de León, E. García Mendoza, I. Estrada, Y. Toledano-Magaña, H. Tiznado,

M. Ovalle-Marroquin, A.G. Soto-Ramos, A. Blanco, Green synthesis of silver nanoparticles using lysiloma acapulcensis exhibit high-antimicrobial activity, Sci. Rep. 10 (1) (2020) 12805, https://doi.org/10.1038/s41598-020-69606-7.
[2] A.W. Khan, N.S. Lali, F.Y. Sabei, M.I. Irfan, M. Naeem-ul-Hassan, M. Sher, A.Y. Safhi, A. Alsalhi, A.H. Albariqi, F. Kamli, Sunlight-assisted green synthesis of gold nanocubes using horsetail leaf extract: a highly selective colorimetric sensor for pb2+, photocatalytic and antimicrobial agent, J. Environ. Chem. Eng. 12 (3) (2024) 112576, https://doi.org/10.1016/j.jece.2024.112576.
[3] S. Ullah, M. Shaban, A.B. Siddique, A. Zulfiqar, N.S. Lali, M. Naeem-ul-Hassan, M.I. Irfan, M. Sher, M.F. ur Rehman, A. Hanbashi, Greenly synthesized zinc oxide nanoparticles: an efficient, cost-effective catalyst for dehydrogenation of formic acid and with improved antioxidant and phyto-toxic properties, J. Environ. Chem. Eng. 12 (5) (2024) 113350, https://doi.org/10.1016/j.jece.2024.113350.
[4] E.N. Alkhafaji, Synthesis and characterization of ag nanoparticle inter nickel/aluminum-layer double hydroxide nano hybrids compounds, IOP Conf. Ser. Mater. Sci. Eng. 871 (1) (2020) 012021, https://doi.org/10.1088/1757-899X/871/1/012021.
[5] S.S. Salem, E.F. El-Belely, G. Niedbała, M.M. Alnoman, S.E.-D. Hassan, A.M. Eid, T.I. Shaheen, A. Elkelish, A. Fouda, Bactericidal and in-vitro cytotoxic efficacy of silver nanoparticles (ag-nps) fabricated by endophytic actinomycetes and their use as coating for the textile fabrics, Nanomaterials Basel 10 (10) (2020) 2082, https://doi.org/10.3390/nano10102082.
[6] R. Hassanien, D.Z. Husein, M.F. Al-Hakkani, Biosynthesis of copper nanoparticles using aqueous tilia extract: antimicrobial and anticancer activities, Heliyon 4 (12) (2018) e01077, https://doi.org/10.1016/j.heliyon.2018.e01077.
[7] H.A. Widatalla, L.F. Yassin, A.A. Alrasheid, S.A.R. Ahmed, M.O. Widdatallah, S.H. Eltilib, A.A. Mohamed, Green synthesis of silver nanoparticles using green tea leaf extract, characterization and evaluation of antimicrobial activity, Nanoscale Adv. 4 (3) (2022) 911−915, https://doi.org/10.1039/D1NA00509J.
[8] N. Ullah, A. Ullah, S. Rasheed, Green synthesis of copper nanoparticles using extract of dicliptera roxburghiana, their characterization and photocatalytic activity against methylene blue degradation, Lett. App.l NanoBioSci. 9 (2020) 897−901, https://doi.org/10.33263/LIANBS91.897901.
[9] W.-R. Li, T.-L. Sun, S.-L. Zhou, Y.-K. Ma, Q.-S. Shi, X.-B. Xie, X.-M. Huang, A comparative analysis of antibacterial activity, dynamics, and effects of silver ions and silver nanoparticles against four bacterial strains, Int. Biodeterior. Biodegradation 123 (2017) 304−310, https://doi.org/10.1016/j.ibiod.2017.07.015.
[10] R. Nivetha, A. Sajeev, A.M. Paul, K. Gothandapani, S. Gnanasekar, P. Bhardwaj, G. Jacob, R. Sellappan, V. Raghavan, S. Pitchaimuthu, Cu based metal organic framework (cu-mof) for electrocatalytic hydrogen evolution reaction, Mater. Res. Express 7 (11) (2020) 114001, https://doi.org/10.1088/2053-1591/abb056.
[11] A. Alizadehdakhel, A. Golzary, An environmental friendly process for extraction of active constituents from herbal plants, Environ. Energy Econ. Res. 4 (1) (2020) 69−81, https://doi.org/10.22097/eeer.2020.198937.1106.
[12] S.B. Aziz, R.B. Marif, M. Brza, A.N. Hassan, H.A. Ahmad, Y. A. Faidhalla, M. Kadir, Structural, thermal, morphological and optical properties of peo filled with biosynthesized ag nanoparticles: new insights to band gap study, Results Phys. 13 (2019) 102220, https://doi.org/10.1016/j.rinp.2019.102220.
[13] F. Farhadi, R. Avan, A. Sahebkar, S. Eghbali, A comprehensive review on eremurus species: Phytochemistry, pharmacology and traditional uses, Phytochem. Lett. 53 (2023) 142−149, https://doi.org/10.1016/j.phytol.2022.12.002.
[14] A.M. Muslim, I.S. Naji, Green synthesis of cuo nanoparticles mediated rhazya stricta plant leaves extract characterization and evaluation of their antibacterial and anticancer activity (in vitro study), Iraq. J. Phys. 22 (3) (2024) 93−105, https://doi.org/10.30723/ijp.v22i3.1259.
[15] A. Jabbar, A. Abbas, N. Assad, M. Naeem-ul-Hassan, H. A. Alhazmi, A. Najmi, K. Zoghebi, M. Al Bratty, A. Hanbashi, H.M. Amin, A highly selective hg 2+ colorimetric sensor and antimicrobial agent based on green synthesized silver nanoparticles using equisetum diffusum extract, RSC Adv. 13 (41) (2023) 28666−28675, https://doi.org/10.1039/D3RA05070J.
[16] N. Assad, M. Naeem-ul-Hassan, M. Ajaz Hussain, A. Abbas, M. Sher, G. Muhammad, Y. Assad, M. Farid-ul-Haq, Diffused sunlight assisted green synthesis of silver nanoparticles using cotoneaster nummularia polar extract for antimicrobial and wound healing applications, Nat. Prod. Res. 39 (8) (2025) 2203−2217, https://doi.org/10.1080/14786419.2023.2295936.
[17] J. Shanmugapriya, C. Reshma, V. Srinidhi, K. Harithpriya, K. Ramkumar, D. Umpathy, K. Gunasekaran, R. Subashini, Green synthesis of copper nanoparticles using withania somnifera and its antioxidant and antibacterial activity, J. Nanomater. 2022 (1) (2022) 1−9, https://doi.org/10.1155/2022/7967294.
[18] M. Rai, A. Yadav, A. Gade, Silver nanoparticles as a new generation of antimicrobials, Biotechnol. Adv. 27 (1) (2009) 76−83, https://doi.org/10.1016/j.biotechadv.2008.09.002.
[19] J.R. Morones, J.L. Elechiguerra, A. Camacho, K. Holt, J. B. Kouri, J.T. Ramírez, M.J. Yacaman, The bactericidal effect of silver nanoparticles, Nanotechnology 16 (10) (2005) 2346, https://doi.org/10.1088/0957-4484/16/10/059.
[20] K. Chaloupka, Y. Malam, A.M. Seifalian, Nanosilver as a new generation of nanoproduct in biomedical applications, Trends Biotechnol. 28 (11) (2010) 580−588, https://doi.org/10.1016/j.tibtech.2010.07.006.
[21] A. Shah, S. Akhtar, F. Mahmood, S. Urooj, A.B. Siddique, M. I. Irfan, M. Naeem-ul-Hassan, M. Sher, A. Alhoshani, A. Rauf, Fagonia arabica extract-stabilized gold nanoparticles as a highly selective colorimetric nanoprobe for cd2+ detection and as a potential photocatalytic and antibacterial agent, Surf. Interfaces 51 (2024) 104556, https://doi.org/10.1016/j.surfin.2024.104556.
[22] A. Ejaz, Z. Mamtaz, I. Yasmin, M. Shaban, A.B. Siddique, M. I. Irfan, A. Ali, S. Muhammad, M.Y. Sameeh, A. Abbas, Cyperus scariosus extract based greenly synthesized gold nanoparticles as colorimetric nanoprobe for ni2+ detection and as antibacterial and photocatalytic agent, J. Mol. Liq. 393 (2024) 123622, https://doi.org/10.1016/j.molliq.2023.123622.
[23] X. Fan, L.H. Yahia, E. Sacher, Antimicrobial properties of the Ag, Cu nanoparticle system, Biology Basel 10 (2) (2021) 137, https://doi.org/10.3390/biology10020137.
[24] P.K. Stoimenov, R.L. Klinger, G.L. Marchin, K.J. Klabunde, Metal oxide nanoparticles as bactericidal agents, Langmuir 18 (17) (2002) 6679−6686, https://doi.org/10.1021/la0202374.
[25] G. Ren, D. Hu, E.W. Cheng, M.A. Vargas-Reus, P. Reip, R. P. Allaker, Characterisation of copper oxide nanoparticles for antimicrobial applications, Int. J. Antimicrob. Agents 33 (6) (2009) 587−590, https://doi.org/10.1016/j.ijantimicag.2008.12.004.
[26] A. Ali, M. Petrů, M. Azeem, T. Noman, I. Masin, N. Amor, J. Militky, B. Tomková, A comparative performance of antibacterial effectiveness of copper and silver coated textiles, J. Ind. Text 53 (2023) 1−36, https://doi.org/10.1177/15280837221134990.
[27] P. Senthilkumar, G. Yaswant, S. Kavitha, E. Chandramohan, G. Kowsalya, R. Vijay, B. Sudhagar, D.R.S. Kumar, Preparation and characterization of hybrid chitosan-silver nanoparticles (chi-ag nps); a potential antibacterial agent, Int. J. Biol. Macromol. 141 (2019) 290−298, https://doi.org/10.1016/j.ijbiomac.2019.08.234.
[28] E.A. Mohamed, Green synthesis of copper & copper oxide nanoparticles using the extract of seedless dates, Heliyon 6 (1) (2020) e03123, https://doi.org/10.1016/j.heliyon.2019.e03123.

[29] M.H. Ali, M.A.K. Azad, K. Khan, M.O. Rahman, U. Chakma, A. Kumer, Analysis of crystallographic structures and properties of silver nanoparticles synthesized using pkl extract and nanoscale characterization techniques, ACS Omega 8 (31) (2023) 28133−28142, https://doi.org/10.1021/acsomega.3c01261.
[30] Y.Y. Loo, B.W. Chieng, M. Nishibuchi, S. Radu, Synthesis of silver nanoparticles by using tea leaf extract from camellia sinensis, Int. J. Nanomed. 7 (2012) 4263−4267, https://doi.org/10.2147/IJN.S33344.
[31] S. Jaast, A. Grewal, Green synthesis of silver nanoparticles, characterization and evaluation of their photocatalytic dye degradation activity, Curr. Res. Green Sustain. Chem. 4 (2021) 100195, https://doi.org/10.1016/j.crgsc.2021.100195.
[32] M.A. Messih, M. Ahmed, A. Soltan, S.S. Anis, Synthesis and characterization of novel ag/zno nanoparticles for photocatalytic degradation of methylene blue under uv and solar irradiation, J. Phys. Chem. Solids 135 (2019) 109086, https://doi.org/10.1016/j.jpcs.2019.109086.
[33] Y.Q. Almajidi, Z.H. Mahdi, N.K. Maraie, Preparation and in vitro evaluation of montelukast sodium oral nanoemulsion, Int. J. Appl. Pharm. 10 (5) (2018) 49−53, https://doi.org/10.22159/ijap.2018v10i5.28367.
[34] A. Moumen, B. Hartiti, P. Thevenin, M. Siadat, Synthesis and characterization of cuo thin films grown by chemical spray pyrolysis, Opt. Quant. Electron. 49 (2) (2017) 70, https://doi.org/10.1007/s11082-017-0910-1.
[35] S. Ullah, R. Khalid, M.F. Rehman, M.I. Irfan, A. Abbas, A. Alhoshani, F. Anwar, H.M. Amin, Biosynthesis of phytofunctionalized silver nanoparticles using olive fruit extract and evaluation of their antibacterial and antioxidant properties, Front. Chem. 11 (2023) 1202252, https://doi.org/10.3389/fchem.2023.1202252.
[36] S. Amin, M. Sher, A. Ali, M.F. Rehman, A. Hayat, M. Ikram, A. Abbas, H.M. Amin, Sulfonamide-functionalized silver nanoparticles as an analytical nanoprobe for selective ni (ii) sensing with synergistic antimicrobial activity, Environ. Nanotechnol. Monit. Manag. 18 (2022) 100735, https://doi.org/10.1016/j.enmm.2022.100735.
[37] M.I. Irfan, F. Amjad, A. Abbas, M.F.U. Rehman, F. Kanwal, M. Saeed, S. Ullah, C. Lu, Novel carboxylic acid-capped silver nanoparticles as antimicrobial and colorimetric sensing agents, Molecules 27 (11) (2022) 3363, https://doi.org/10.3390/molecules27113363.
[38] N. Babayevska, Ł. Przysiecka, I. Iatsunskyi, G. Nowaczyk, M. Jarek, E. Janiszewska, S. Jurga, Zno size and shape effect on antibacterial activity and cytotoxicity profile, Sci. Rep. 12 (1) (2022) 8148, https://doi.org/10.1038/s41598-022-12134-3.